



Cite this: *Green Chem.*, 2022, **24**, 2962

Spruce bark stilbenes as a nature-inspired sun blocker for sunscreens[†]

Jinze Dou, Mengmeng Sui,^a Kiia Malinen,^a Terhi Pesonen,^b Tiina Isohanni^b and Tapani Vuorinen^a

Stilbene glucosides are a class of natural compounds that have been used as natural antioxidants and anti-fungal and antibacterial agents. Here, spruce bark extract, rich in stilbene glucosides, was used as a natural ultraviolet-protective additive for sunscreens. The ultrasound-assisted extraction of fresh Norway spruce (*Picea abies*) inner bark with 60% ethanol provided an extract in ca. 25% yield, of which one third consisted of three stilbene glucosides (astragin, isorhapontin and polydatin) which were fully characterized and quantified by 1D and 2D NMR spectroscopy and high resolution-liquid chromatography mass spectrometry (HR-LC/MS). Emulsions of the extract were prepared and applied on polymethyl methacrylate (PMMA) plates to study the effect of the extract on UV light absorbance. A 10% emulsion with spruce crude extracts (containing 35% stilbene glucosides) alone provided UV protection equal to half the efficiency of commercial SPF 15 sun lotions, which also displayed a 21–32% higher SPF effect in comparison with the same dosages of alkali lignin nanoparticles using the same sunscreen emulsification process. A preparative scale chromatography was established for the first time as a fast and highly efficient method in the small-scale recovery of stilbene glucosides from spruce inner bark for full structural elucidation and has a good chance to be industrially scalable. Overall, this exploration may launch a new era for the application of stilbene glucosides of spruce bark extracts as genuine replacements for synthetic UV filters, upgrading this underappreciated bark residue from energy production to higher value cosmetic use.

Received 21st January 2022,
Accepted 28th February 2022

DOI: 10.1039/d2gc00287f

rsc.li/greenchem

Introduction

Ultraviolet (UV) radiation (particularly 290–400 nm) exposure plays a key role in the development of viral skin diseases. Such a state is partially caused by the depletion of the defence and immune systems of the skin.¹ Most chemical sunscreen products are used to block UV rays before penetrating through the skin. However, the side-effects (toxicity and phototoxicity)^{2,3} of some chemically derived UV filters have recently been reported as listed in Table 1, for example, benzophenone derivatives are found to be cytotoxic in nature causing an apoptosis-inducing effect,⁴ octyl methoxycinnamate is reported to decrease cell viability and increase the apoptosis against the neuroblastoma cell line,^{5,6} and *para*-aminobenzoic acid can cause photoallergic reactions.⁷ Moreover, approximately 6000–14 000 tons per year of sunscreens⁸ pose a threat to marine ecosystems, and thus some countries have started banning sunscreens containing certain chemical additives. Furthermore, the benefits of

natural sunscreens are also fuelled by the increasing awareness of sustainability; however, the allowed UV filters are restricted due to tighter regulations over growing public health concerns.

The radiation protection performance of natural UV additives, such as leaves of aloe vera, green tea, and soybean oil,⁹ is listed in Table 1. However, their supply chain may not be as sustainable as wood (spruce needles¹⁰ or lignin^{11,12}) because renewable wood can be sustainably harvested by the pulping industry throughout the season. Furthermore, the sunscreen demand is growing in double digit percentages globally nowadays; thus we need to develop alternative, innovative and safer new types of naturally derived UV-filter ingredients urgently to overcome the side effects (toxicity and phototoxicity) of some chemically derived UV filters. Pentacyclic triterpenoids from the birch bark, particularly betulin,¹³ have been the development focus as novel pharmacological ingredients for their known antitumor and anti-inflammatory activities. The launch of innomost^{TM 14} has gained attention for transforming 100% pure bioactive azelaic acid from birch bark for the first time as anti-acne and anti-rosacea¹⁵ ingredients in personal care formulation products. Norway spruce (*Picea abies*) is another major raw material of the European forest industry, and in Finland alone approximately 0.9–1.3 million tons of spruce bark are annually used for energy production.¹⁶ Spruce bark

^aDepartment of Bioproducts and Biosystems, Aalto University, Espoo, Finland.
E-mail: jinze.dou@aalto.fi; Tel: +358 413115001

^bLasikuja 2, Lumene Oy, Espoo, Finland

† Electronic supplementary information (ESI) available. See DOI: 10.1039/d2gc00287f



Table 1 Summary of the toxic effects (or function mechanism) from several selected artificial and natural photoprotective compounds

	Concerned chemicals (or plant, wood)	Action spectrum	Toxic effects (artificial) or function mechanism (natural)	Ref.
Artificial	<i>Organic UV filters</i>			
	Octyl methoxycinnamate	UVB	Decreased cell viability and increased apoptosis against neuroblastoma cell line	5 and 6
	Benzophenone	UVA/UVB	Apoptosis-inducing effect against human leukemia cell lines	4 and 5
	<i>para</i> -Aminobenzoic acid	UVB	Photoallergic reactions on the skin	5
	Camphor derivative	UVB	Impaired preceptive, cell viability and receptive sexual behaviour	5
	Octocrylene	UVA/UVB	Impaired expression of genes related to metabolism in brain	5
	<i>Inorganic filters</i>			
Natural	Zinc oxide particles	UVA/UVB	Disrupted ion homeostasis and oxidative stress	5
	<i>Plant derived</i>			
	Leaves of aloe vera	UVA/UVB	Generated metallothionein reduces the production and release of skin keratinocyte-derived immunosuppressive cytokines	3 and 19
	Green tea	UVA/UVB	Antioxidant activities from polyphenols, caffeine, flavonoids, etc.	3 and 19
	Soybean oil	UVA/UVB	Antioxidant vitamin E reduces the photooxidative damage	3 and 19
	<i>Wood derived</i>			
	Lignin	UVA/UVB	Antioxidant property of lignin	11 and 12
	Spruce bark extracts	UVA/UVB	Radical scavenging and antioxidant activity of the stilbene glucosides	Present study

contains a variety of stilbene glucosides (*ca.* 10–20 wt%), which are mainly present in the phloem (inner bark). Its stilbene content depends mainly on the harvest season, geographic location, and position in the tree.^{17,18} By rough calculation, 36 000–52 000 tons of stilbene are currently wasted particularly during the storage and debarking stages at the Finnish pulp mill every year, which in turn adversely affects the chemical oxygen demand (COD) of the mill, and then the associated wastewater treatment requires additional cost from the pulp mill.

Stilbene glucosides are secondary metabolites and have been shown to be effective in a tree's defence mechanism as a natural counteragent to fungal pathogens,²⁰ oxidative stress and aging-related diseases,^{21,22} and Alzheimer's disease.²³ These hydroxystilbene glucosides have also been reported to be incorporated into lignin's structure through β -ether bonds in Norway spruce bark.²⁴ Astringin, the major stilbene in spruce bark extracts (Fig. 1), has significant radical scavenging and antioxidant activities.²⁵ Polydatin can also reportedly be used to potentiate chemotherapy for human colon cancer.²⁶ Resveratrol, the aglycone of polydatin, is the best-known stilbene compound for its multi-spectrum pharmacological activities (e.g., antioxidant, anti-aging, and antimicrobial activities, and treatment of neurodegenerative disease).²⁷

Although many established pharmaceutical and biological activities have been reported for spruce bark stilbene compounds, their poor solubility and stability in water^{28–30} limit

their maximal extraction efficiency from spruce bark, thus preventing their use as value-added biochemicals. A high partition coefficient ($\log P$)²⁹ of *trans*-stilbene suggests that stilbene compounds are hydrophobic, and therefore, extraction with water alone cannot achieve a satisfactory yield. Several studies have reported that the addition of a polar organic solvent (e.g., acetone or ethanol, Table 2) could lead to a marked increase in stilbene's solubility. The aqueous solution of stilbene glucosides is sensitive to light and temperature³¹ although Soural *et al.*³² claimed accelerated solvent extraction at a temperature of 100 °C in methanol as an efficient method for the extraction of stilbenes from grape cane. *trans*- and *cis*-Stilbenes occur as stereoisomers, but *trans*-isomers mostly exist in nature due to their relatively high thermodynamic stability. The *trans*-stilbene glucosides may convert into their *cis*-isomers under light and further into phenanthrene under UV irradiation.³³ Ultrasound-assisted extraction (UAE)^{34,35} is a commonly used technique in herbal extraction with the following advantages: high production efficiency, fast mass transfer, low energy consumption and high scalability.

The objective of this study was to optimize the extraction process of stilbene glucosides using mixtures of water and ethanol, a solvent that is derived from biomass, and to characterize the chemical composition of the optimized extract using advanced nuclear magnetic resonance (NMR) spectroscopy and liquid chromatography–mass spectrometry (LC-MS) techniques. Although there have been cases applying spruce bark

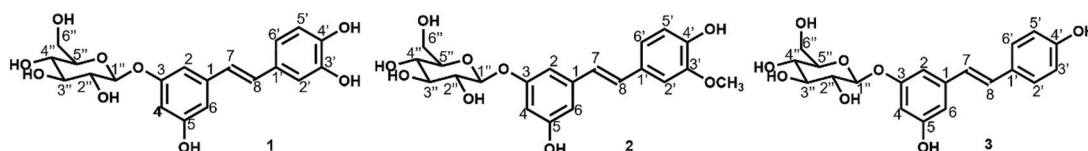


Fig. 1 Main stilbene glucosides of Norway spruce bark: 1 astringin (CAS number 29884-49-9; solubility in water: 0.73 g L⁻¹ (predicted, TMIC ID: FDB008433); pK_a 8.99); 2 isorhapontin (32727-29-0; pK_a 9.16); 3 polydatin (27208-80-6; solubility in water: 1.26 g L⁻¹,²⁸ pK_a 9.21).



Table 2 Solvents used in extracting stilbene glucosides (or their aglycones) from Norway spruce (inner) bark^{17,18,20,36}

Main extracted component	Section	Age (a); harvesting month	Solvent; liquid-to-solid ratio (ml g ⁻¹)	Temperature (°C); time (min)	Yield (%)	Analysis	Ref.
Stilbene glucosides	Bark	51–82; April, June	Acetone; 30 : 1	56; 360	0.5–8.3	GC-MS; HPLC	18
Stilbene glucosides, stilbenes	Inner bark	31; September	Acetone–water (9 : 1); 3 : 1	100; 15	10.8	GC-FID	36
Stilbene glucosides	Bark	18, 37; unknown	Acetone–water (95 : 5); 100 : 1	RT; 30	2.7–4.8	GC-FID	17
Stilbene glucosides, stilbenes	Bark	unknown	Ethanol–water (85 : 15); 10 : 1	60; 120	1.8	HPLC-MS; NMR	20
Stilbene glucosides	Inner bark	50; March	Ethanol–water (60 : 40); 30 : 1	45; 20	8.96	NMR	Present study

Gas chromatography-mass spectrometry (GC-MS); high-performance liquid chromatography (HPLC); gas chromatography with flame ionization detection (GC-FID); nuclear magnetic resonance spectroscopy (NMR); and liquid chromatography-mass spectrometry (LC-MS).

trans-resveratrol for photoaging protection of human skin and hair masks from IFF Lucas Meyer CosmeticsTM³⁷ and SkinScienceTM,³⁸ the composition of the spruce bark extracts and its correlation with the UV blocking activity has not been investigated yet. The stilbene-rich fraction of spruce bark was used as a UV blocker in sunscreens in a preliminary study,³⁹ and a follow-up study has been systematically conducted for the first time to (1) develop an industrially scalable preparative chromatographic purification process for stilbene glucosides and evaluate the full chemical profile of the spruce bark extracts and (2) evaluate their use as UV blockers in sunscreens using *in vitro* sun protection factor (SPF) measurements on polymethyl methacrylate (PMMA) plates.

Materials and methods

Raw materials and chemicals

Fifty-year old spruce stems were harvested from a farm in Lempäälä, Finland, on 6 March 2017. The inner bark was manually stripped from the spruce stems on 13 March 2017. The collected spruce inner bark was freeze-dried and ground into 1 mm sized particles. The samples were stored in aluminium foil at –20 °C before further use. Sulfuric acid (purity: 98%), gradient-grade acetonitrile (99.9%), acetone (99.9%), *n*-hexane, ethanol (99.5%), astringin, polydatin, isorhapontin, DMSO-*d*6 and pyridine-*d*5 were supplied by Sigma Aldrich, Finland. Resveratrol was supplied by Evolva Holding SA (Reinach, Switzerland). The original non-modified finished sunscreen lotion used here was a Lumene Nordic Hydra 24 h moisturizer (50 mL) (base-L). Commercial sunscreen lotions were Lumene Day Cream SPF 15 (SPF 15-L), Day Fluid SPF 30 (SPF 30-L), and Biotherm Skin Oxygen Cream SPF 15 (SPF 15-B). All these commercial creams were supplied by Lumene Oy (Fig. S1†).

Experimental procedures

Ultrasound-assisted extraction (UAE). Prior to UAE, the milled spruce inner bark (IB) was pre-treated with *n*-hexane at 75 °C for 15 min to remove the lipophilic extracts (Fig. 2). The

n-hexane treated IB was collected and dried at 40 °C overnight and stored at –20 °C for further analysis. UAE extraction was performed with an ultrasonic cleaner USC 600 TH (Avantor, Pennsylvania) under the following conditions: solvent: water or 60% ethanol (v/v); liquid-to-solid ratio: 30 : 1 ml g⁻¹; temperature: 45–75 °C; and time: 5–60 min. All extractions were conducted using aluminium foil for light protection. The extracts were filtered into crucibles (16–40 µm) and oven-dried overnight at 40 °C. The lyophilized UAE extracts were stored in amber-coloured glass containers to avoid exposure to light and air. For a preliminary stability study, one set of UAE extracts was prepared at 45 °C in a series of time periods (5 to 45 min) and then stored exposed to open air and light for six weeks.

Emulsification. Two different emulsification preparations were carried out during the study. First, creams of 1–10 wt% spruce inner bark extract (SBE) were prepared in aluminium foil covered jars by applying simple magnetic stirring at room temperature (emulsification I). For example, a 1 wt% SBE sunscreen was prepared by blending SBE (0.02 g) with base-L (1.98 g) at 600 rpm overnight. The lotions were named E-I-1%, E-I-2%, E-I-5%, and E-I-10% according to their SBE content. The second emulsification (emulsification II) followed the traditional protocol:⁴⁰ heating, melting, and mixing with a high shear mixer (Fig. 2). The oil phase (C) and water phase (B) were separately heated to 80 °C, combined, and homogenized with a high shear mixer, followed by introducing the water phase (A) with 1–2 wt% SBE and mixing again to achieve a homogeneous lotion. The pH of the lotion was finally adjusted to neutral before storing it in a sealed tube for further UVP measurements. The detailed compositions of the water phase B and oil phase C are listed in Table S1.†

Purification through preparative-scale liquid chromatography. Fraction collection (Fig. S2 and Table S2†) was performed using a system from Shimadzu consisting of two LC-20AP pumps, a degasser, an SIL-10AP autosampler, an SPD-M20A diode array detector, and an FRC-10A fraction collector. A semi-preparative Luna® Omega 5 µm PS C18 100 Å (250 × 10 mm) column and a Kinetex® 5 µm Biphenyl 100 Å (250 × 10 mm) column were used as a coupled column system (Table S2†) for the separation. The spruce bark extract with a





Fig. 2 Illustration of various steps and materials in the experimental work. The originally light-colored inner bark turned reddish brownish by the action of light and atmospheric oxygen. The *in vitro* UV protection (UVP) was evaluated by UV absorbance measurements of the creams.

concentration of 59.37 mg ml⁻¹ was dissolved in an acetonitrile–water mixture (60:40). The injection was performed using an injection volume of 50 µl. Separation of sugars, astringin, polydatin, isorhapontin, *etc.* was achieved using a gradient of acetonitrile (solvent B) and ultra-pure water (solvent A) at a flow rate of 3 mL min⁻¹. The gradient was set as follows: solvent A was held at 90% for 12 min followed by a linear gradient from 90% solvent A to 80% in 1 min. Then solvent A was held at 80% for 47 min followed by a linear gradient from 80% solvent A to 70% in 1 min. Solvent A was held at 70% for 39 min followed by a linear gradient from 70% solvent A to 0% in 1 min. Solvent A was held at 0% for 19 min before increasing back to 90%. Nine fractions were continuously quantitatively collected from 19 injections with detection wavelengths of 210 and 320 nm. All organic solvents were removed from the collected fractions using a rota-vapor (Büchi Labortechnik AG) and the remaining fractions were freeze-dried for recovery yield calculations and structural analysis.

Analytical techniques

In vitro SPF measurements. The emulsified sunscreen lotion was evenly spread onto the PMMA plate (1.3 mg cm⁻²) using a gloved finger before being placed in a 30 °C oven (Model ED 115, BINDER) in the dark for 5 min. The UV absorbance spectrum of the PMMA plate (containing the spread product) was measured at 290–400 nm using a Kontron 933 spectrophotometer equipped with an integrating sphere to determine the SPF and UVA protection, and calculate the critical wavelength (CW). The PMMA plates (containing the spread product) were then irradiated for a period of 10 min under a solar simulator (SUNTEST CPS+, Atlas Material Testing Technology) producing a dose of 2 DEM (400 J m⁻²), which was used to mimic sun exposure to determine the photostability of the tested creams.

The absorbance of the sample was measured again over the range of 290–400 nm after irradiation and 30 °C drying. Four independent measurements were carried out to increase the reliability of the data.^{11,41,42}

The sun protection factor (*in vitro*) is expressed as SPF *in vitro* using an expression where $E(\gamma)$ refers to the action spectrum of erythema, $S(\gamma)$ is the standard solar spectrum, $T(\gamma)$ is the average transmission of the layer of the tested product spread on the PMMA plate, and $d(\gamma)$ is the wavelength interval (1 nm). The SPF *in vitro* was calculated using the following eqn (1):

$$\text{SPF } \textit{in vitro} = \sum_{290}^{400} E(\gamma)S(\gamma)d(\gamma) / \sum_{290}^{400} E(\gamma)S(\gamma)T(\gamma)d(\gamma). \quad (1)$$

The *in vitro* assessment of the UVA protection factor (PF-UVA) is expressed from the entire residual UVA spectrum that has passed through the sample layer. The value is obtained by including the calculation mode of the efficiency of the Persistent Pigmentation Darkening (PPD) for wavelengths between 320 nm and 400 nm. A xenon arc lamp is used to ensure a sufficient level of irradiance and to not induce wrongly the photostability of the product, where $P(\gamma)$ refers to the action spectrum of PPD, $L(\gamma)$ is the spectrum of the xenon arc lamp, $T(\gamma)$ is the average transmission of the layer of the test product spread on the PMMA plate, and $d(\gamma)$ is the wavelength interval (1 nm). The PF UVA was calculated using the following eqn (2):

$$\text{PF UVA} = \sum_{320}^{400} P(\gamma)L(\gamma)d(\gamma) / \sum_{320}^{400} P(\gamma)L(\gamma)T(\gamma)d(\gamma). \quad (2)$$

Nuclear magnetic resonance (NMR) spectroscopy. One-dimensional ¹H and ¹³C and two-dimensional ¹H–¹³C heteronuclear single quantum coherence (HSQC) spectra were



acquired with a 400 MHz Bruker Avance III spectrometer using DMSO-*d*6/pyridine-*d*5 (4:1) as the solvent.^{43,44} 1,3,5-trioxane (δ C 93.1, δ H 5.12 ppm) and DMSO (δ C 39.5, δ H 2.49 ppm) were used as internal standards for stilbene glucoside quantification and chemical shift calibration, respectively. HSQC spectra were acquired (spectral widths of 15 ppm and 250 ppm for 1 H and 13 C, respectively) using a relaxation delay (d_1) of 2 s, 1 K data points, 256 t_1 increments, and 100 transients. An adiabatic version of the HSQC experiment was used (hsqcetgpsp.2 pulse sequence from the Bruker Library). 1 H NMR was performed using a spectral width of 16 ppm, d_1 of 1.5 s, and 32 K data points. The following parameters were used for 13 C: spectral width of 220 ppm, d_1 of 1.5 s, and 65 K transients of 64 K data points. The spectral images were processed using Topspin 4.0 (Bruker).

Chemical composition. The chemical composition of spruce bark was analysed according to NREL/TP-510-42618.⁴⁵ The quantification of the hydrolysed monosaccharide was performed by high-performance anion-exchange chromatography with pulsed amperometric detection (HPAEC-PAD). The detailed experimental parameters were summarized previously.⁴⁶

Stilbene quantification. A UV-vis spectrophotometer (Shimadzu UV-2550) was used to test the UV absorption (190–400 nm) for both extracts and authentic standards. All samples were diluted to a UV absorbance range of 0.2–0.7. *trans*-Polydatin was used as an external standard for a relatively quick and reliable quantification of stilbene glucosides with the UV-vis spectrometer.⁴⁷ Polydatin, its aglycone piceatannol and the extract (SBE) all showed an absorption maximum at 320 nm.²⁰ A series of 4, 6.2, 7.6, 10 and 11.6 μ g mL⁻¹ of polydatin solutions was used to build a linear calibration line at 320 nm (Fig. S3†).

Liquid chromatography-mass spectrometry. The HPLC-DAD-MS and high-resolution mass spectrometry (HRMS) analyses were conducted using an Agilent 1260 Infinity High Pressure Liquid Chromatography (HPLC) system (Agilent Technologies, Singapore). The HPLC system was coupled with an Agilent diode-array detector (detection wavelengths: 210 nm and 300 nm) and an Agilent 6350 QTOF mass spectrometer (Santa Clara, USA) equipped with a dual electrospray ionization (ESI) interface (Agilent Technologies). Detection was carried out within a mass range of 100–1100 m/z or 100–3200 m/z . The mass accuracy of the instrument using external calibration was specified as \leq 3 ppm. The HPLC separation was performed using Phenomenex Luna® Omega 5 μ m PS C18 100 \AA (150 \times 2.1 mm) and Kinetex® 5 μ m Biphenyl 100 \AA (150 \times 2.1 mm) columns at room temperature using the same gradient program as above (Table S2†). The analysis was performed with a flow rate of 0.20 mL min⁻¹ and an injection volume of 10 μ L. The analytes were measured in negative ion mode and the capillary voltage was set to +4000 V. The drying gas flow was set to 11 L min⁻¹ with a temperature of 300 °C. The nebulizer, fragmentor, skimmer, and octopole RF were set to 30 psi, 160 V, 65 V and 400 V, respectively.

The HRMS analysis of the fractions was performed using the HPLC system as an injector with an injection volume of

5 μ L and a flow rate of 0.250 mL min⁻¹ (50:50 acetonitrile: ultra-pure water). The ionization was performed using a dual electrospray in the negative ion mode. The instrumental parameters were set as follows: capillary voltage: 4500 V, source temperature: 300 °C, drying gas: 11 L min⁻¹, nebulizer pressure: 30 psi, fragmentor: 160 V, skimmer: 65 V and octopole RF: 400 V, respectively. A similar method has been recently reported, combining a supercritical fluid and high-resolution mass spectrometry, having potential for use in qualitative and quantitative determination of lipophilic extracts (such as triglycerides and sterols) from pine bark.^{48,49}

Results and discussion

UAE extraction of spruce bark

To achieve a high extraction efficiency of stilbene glucosides from spruce bark, the effects of the solvent (water or 60 v% of ethanol), temperature (45–75 °C), and time (5–60 min) were studied since the stilbene glucosides are sparingly soluble in water and thermally unstable. Fig. S4† shows the effects of the solvent and temperature on the gravimetric extract yield and the yield of stilbene glucosides in 20 min extraction time. Generally, the gravimetric extract yield increases with the rise of temperature irrespective of the solvent although the use of 60 v% ethanol leads to a higher maximum yield compared to water extraction (28 and 23%, respectively). More importantly, the yield of stilbene glucosides was much higher (11–19%) in 60 v% ethanol than in water (4–6%). Therefore, 60 v% ethanol was selected as the solvent for the subsequent experiments to investigate further the effects of temperature and time on the stilbene glucoside yields.

Although there were some variations in the results, a 20 min extraction time at 45 °C was sufficient to provide the maximum 19% yield of stilbene glucosides (Fig. 3). Application of longer time or higher temperature had possibly an adverse effect on the stilbene glucoside yield although the overall extract yield remained constant. According to a previous study, stilbene glucoside solutions are fairly stable below 60 °C, above which their stability decreases as the aglycones liberate and convert to other phenolic compounds.³¹ Six weeks exposure of the extracts to light showed a significant decrease in the stilbene glucoside content (UV absorption at 320 nm) (Fig. S5†), which was tentatively explained by the light-induced *trans*- to *cis*-isomerization and subsequent formation of phenanthrene structures.³³ These results emphasized the need to carry out the extraction in darkness (with protection with aluminium foil). Further extractions were then carried out with 60 v% ethanol at 45 °C using a 20 min extraction time.

As expected, the extraction with 60 v% ethanol had little or no effect on the non-extractive components of spruce bark (Fig. 4), which consisted mostly of carbohydrates (neutral sugars derived from cellulose, hemicelluloses, pectin, etc.) and lignin. 'Others' refer to substances, such as pectic galacturonic acid, acetyl groups of xylan and tannins, which are not specifically included in the applied analytical protocol.⁴⁵ The treat-



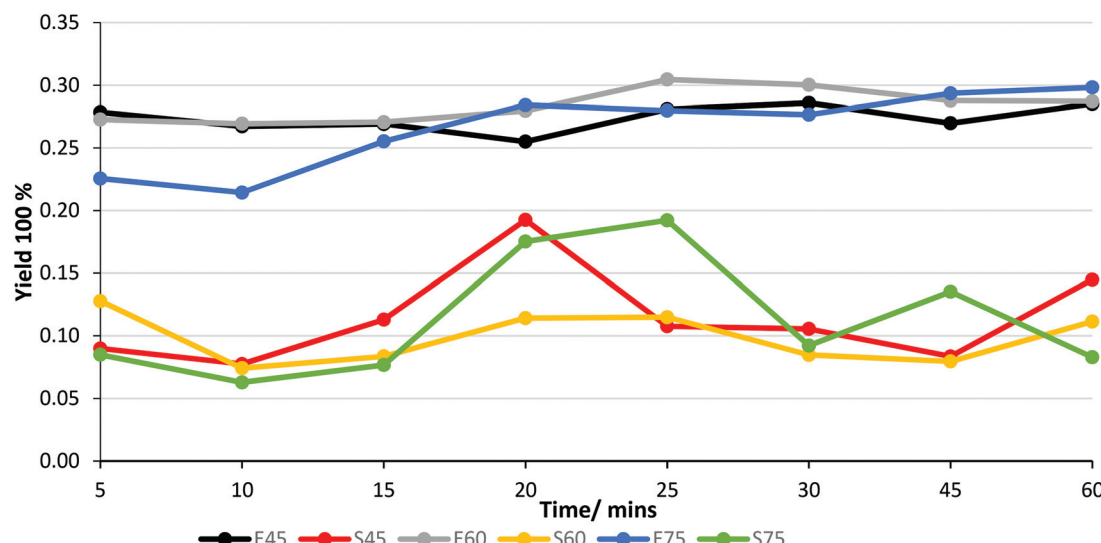


Fig. 3 Effect of temperature (45, 60 and 75 °C as indicated in the legends) and time on gravimetric extract yield (E) and spectrophotometric (320 nm) stilbene glucoside yield (S) from spruce inner bark under UAE extraction.

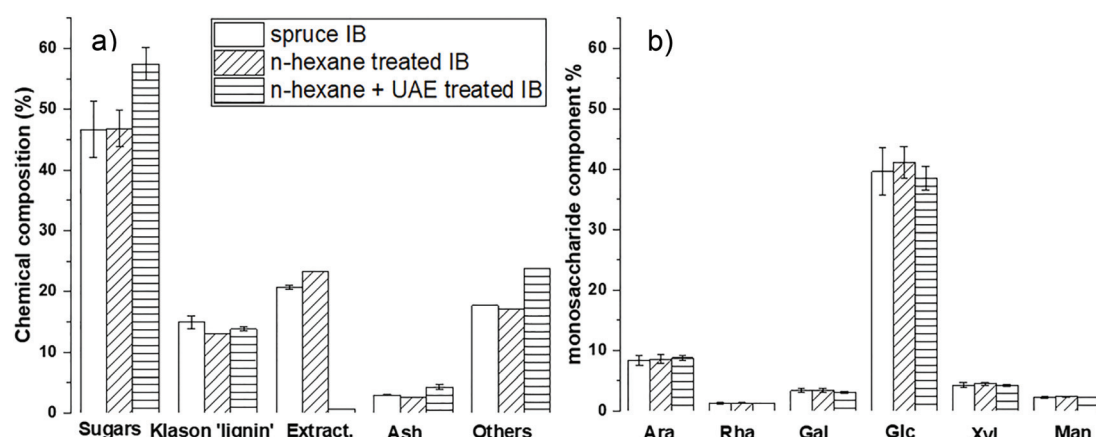


Fig. 4 (a) Overall chemical and (b) carbohydrate composition of spruce inner bark (IB), n-hexane treated IB, and n-hexane + UAE treated IB. Abbreviations: arabinose (Ara), rhamnose (Rha), galactose (Gal), glucose (Glc), xylose (Xyl), and mannose (Man).

ment with 60 v% ethanol removed practically all extracts (>20% of the dry matter) of spruce bark without affecting the other components of the bark.³⁶ In summary, 60 v% ethanol appears to be a practical and sustainable solvent to purify the non-structural stilbene-glucosides with a high yield from the spruce bark within a short time.

Chemical composition of spruce bark extract

A preparative-scale chromatography was designed and implemented to recover stilbene glucosides from spruce bark extracts, and to reveal the complete chemical profile of the spruce bark extracts. As the separation in column chromatography depends on the partition behaviour of the bioactive compounds in relation to the selected resin material,⁵⁰ the separation mechanism between the target molecule and the

introduced resin needs to be modified. The key process design criteria are the high purity and recovery yield, low solvent consumption and a good chance to be industrially scalable. An efficient separation and purification of stilbene glucosides from spruce bark extracts were successfully demonstrated. Although the chemical characterization of stilbene glucosides has been prevalently conducted by deconstructive techniques, such as GC-FID or GC-MS (Table 2), which always require prior derivatization, here structural elucidation by the non-deconstructive spectroscopic (LC-MS and NMR) techniques was successfully used for the structural analysis of both the spruce bark UAE extracts (Fig. 5 and 6) and their each individually purified fractions (Fig. S6–S14†). The NMR signals were assigned based on the literature^{44,51} and NMR spectra of authentic astringin, polydatin, and isorhapontin (Fig. S15–S17†).

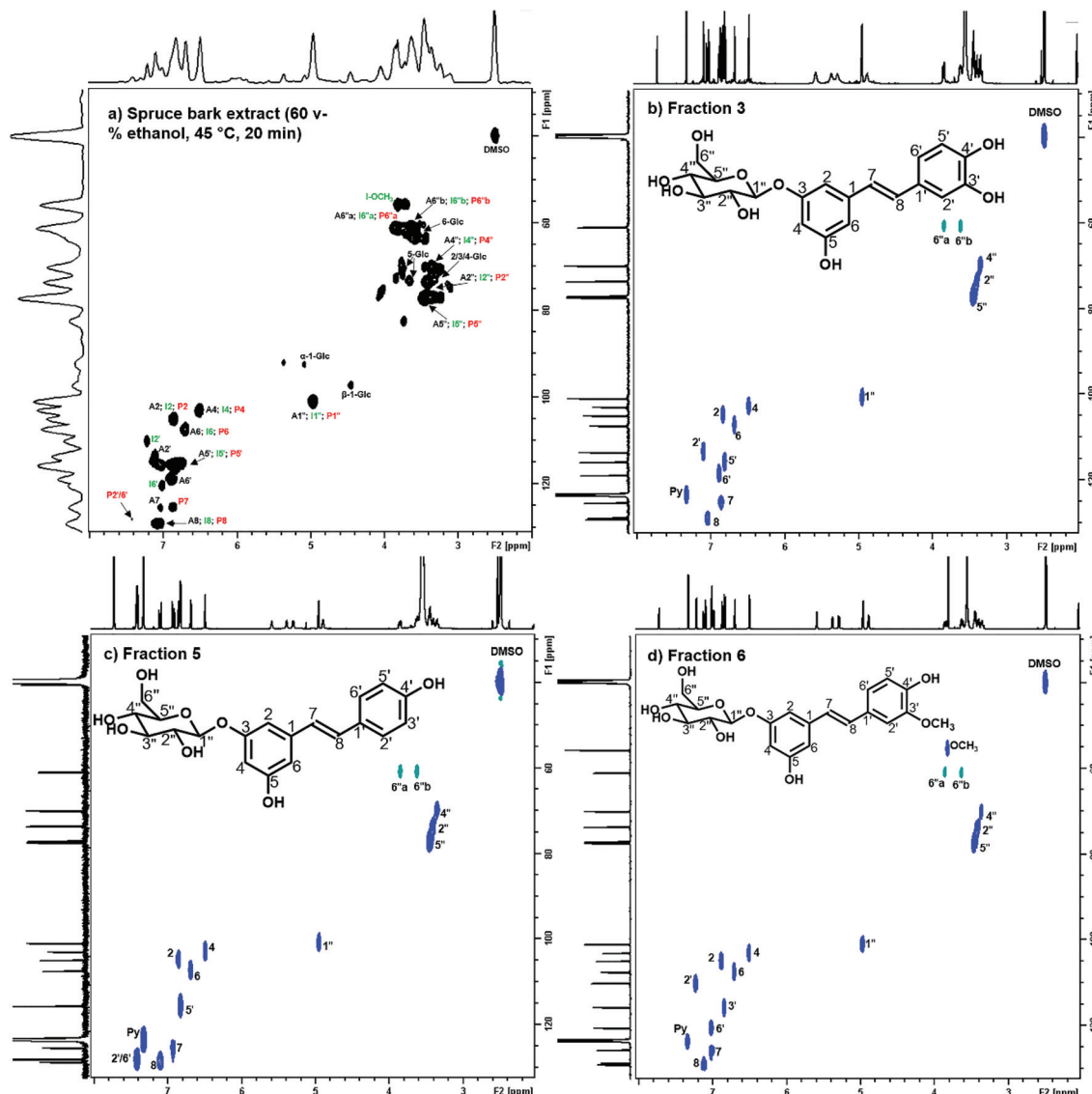


Fig. 5 2D ^1H – ^{13}C HSQC NMR spectrum ($\delta\text{C}/\delta\text{H}$, 29–131/2.0–8.0 ppm) of (a) spruce bark extract (60 v/v ethanol, 45 °C, 20 min); (b) purified fraction 3 (astrin, Fig. S2†); (c) purified fraction 5 (polydatin, Fig. S2†); and (d) purified fraction 6 (isorhapontin, Fig. S2†) in DMSO– d_6 /pyridine– d_5 (v/v 4 : 1). The labels assign the signals from stilbene glucosides astrin (A, black), isorhapontin (I, green) and polydatin (P, red) (Fig. 1) for (a). The chemical shifts of each assigned signal are summarized in Table S3.†

Several unlabelled signals in the anomeric (90–110 ppm) and non-anomeric (60–85 ppm) ^{13}C NMR regions (Fig. 5 and 6), fraction 1 and fraction 2 (Fig. S2, Table S2,† and Table 3) indicated the presence of carbohydrates and catechin (or epicatechin) in the extract. Most chemical shifts of the stilbene glucosides were well resolved and 1,3,5-trioxane was applied as an internal standard for their quantitative determination by ^1H NMR spectroscopy.⁵² The main stilbene glucosides (astrin, isorhapontin and polydatin) accounted for 35.1% of the extract (Table 3) which was approximately one third and half less than what was estimated from the ^1H NMR spectroscopy (46.8%) and UV absorption at 320 nm (75.5%), respectively. The difference might originate from the presence of some polymeric materials, such as condensed tannins, which could

explain the presence of underlying broader signals in the ^1H and ^{13}C NMR spectra (Fig. 6). In fact, the ^{13}C NMR spectra of the bark extracts contained several broad ‘background’ signals at chemical shifts that are characteristic of polymeric condensed tannins⁵³ (Fig. S18†). Other tentatively assigned fractions in Table 3 and Fig. S19† (approx. 50 wt% of spruce bark extracts) included dihydrokaempferol, keto-teracacidin, taxifolin-3-glucoside, and kaempferol 7-O-glucoside which have been previously reported for their presence in spruce bark extracts^{54,55} and could possibly associate with their role in the biosynthesis of spruce phenolic defence against bark beetles.⁵⁴ The overall stilbene glucoside yield was 8.96% of spruce inner bark, which is close to the earlier reported yield (10.8%) in extracting spruce bark with acetone–water (9 : 1 v/v).³⁶



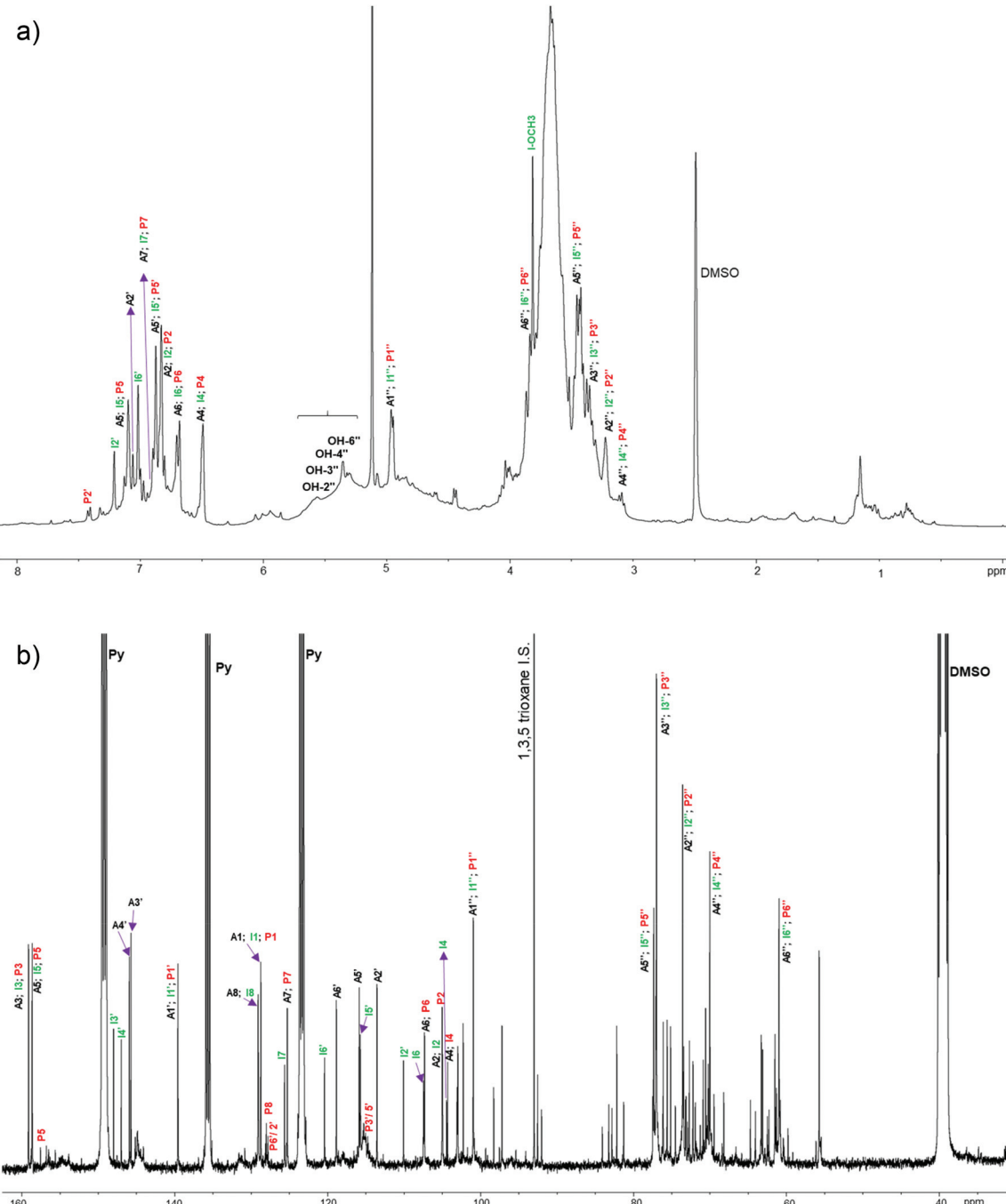


Fig. 6 ^1H (a) and ^{13}C (b) NMR spectra of spruce bark extract (60 v% ethanol, 45 °C, 20 min) in $\text{DMSO-d}_6/\text{pyridine-d}_5$. The labels assign the signals from stilbene glucosides astringin (A, black), isorhapontin (I, green) and polydatin (P, red) (Fig. 1). The chemical shifts of each assigned signal are summarized in Table S3.†

Use of spruce bark extract as a UV blocker

Inspired by its high UV absorptivity, intrinsic brownish colour and the established pharmacological (particularly anti-aging) characteristics,^{20–27} the spruce bark extract was tested for its performance in sunscreens. Two sets of samples (emulsification I and emulsification II) have been prepared more recently and therefore knowledge on their long-term stability is still lacking.

The UV blocking ability of the emulsions was explored by applying them on a PMMA plate and measuring the change in the absorbance of UV light.^{41,42} With 10% addition of SBE (containing 35% pure stilbene glucosides) to pure creams, emulsification I led to a product (E-I-10%) that blocked the UV radiation equal to half the efficiency of commercial SPF 15-L and SPF 15-B (Fig. 7 and Table 4). Logically, adding 10% purified stilbene glucosides to the pure cream is expected to go

Table 3 Mass balance of the spruce bark extract based on the purified fractions (Fig. S2†). Standard deviations are included in parentheses. Tentatively assigned fractions are in italic format. The result interpretation is based on NMR (N), HPAEC-PAD (H), LC-MS (L), and references (in number)

	Component	Analytic (or reference)	Yield ^a %	Yield %
Fraction 1	Glucose; fructose	N; H; L	12.0	2.6 (0.04) ^b
	<i>quinic acid</i>	L	—	—
Fraction 2	Catechin or epicatechin or both	N; L; 51; 52	16.6	—
	<i>dihydrokaempferol or keto-teracacidin</i>	N; L; 51; 52	—	—
Fraction 3	Astringin	N; L	18.9	18.3 (3.1) ^c
Fraction 4	<i>taxifolin-3-glucoside</i>	L; 51	4.5	—
Fraction 5	Polydatin	N; L	2.5	4.2 (2.2) ^d
Fraction 6	Isorhapontin	N; L	13.7	24.7 (1.8) ^e
Fraction 7	$M-H = 507.1861, M_w (\approx 508.1861); M-H = 707.1963, M_w (\approx 708.1963)$	L	4.7	—
Fraction 8	<i>Kaempferol 7-O-glucoside; C₂₁H₃₆O₁₀ or C₂₁H₂₀O₁₁</i>	N; L; 51	11.8	—
Fraction 9	$M-H = 595.1456, MW (\approx 596.1456), C_{30}H_{28}O_{13}; M-H = 375.2913, MW (\approx 376.2913), C_{24}H_{40}O_3$	L	8.9	—
Uncharacterized fractions ^f	Ash	—	—	1.5 (0.1)
	<i>C₁₆H₃₂O₂ and C₁₈H₃₆O₂</i>	L	—	—
Stilbene/overall		35.1/93.7	46.8/49.0	

^a Quantification by nineteen rounds of quantitative fractionation. ^b Quantification by HPAEC-PAD based on three independent measurements.

^c Integration of H_{2'} of astringin and determined by ¹H NMR based on three independent measurements. ^d Integration of H_{2'} from polydatin and determined by ¹H NMR based on three independent measurements. ^e Integration of CH₃O and H_{2'} from isorhapontin and determined by ¹H NMR based on three independent measurements. ^f May include C₁₆H₃₂O₂, C₁₈H₃₆O₂, condensed tannins, ash, etc.

above the UV blocking efficiency of the commercial SPF 15 lotions. In comparison with alkali lignin nanoparticles,¹¹ SBE provided a 21–32% higher SPF effect than with the same dosages of 5 wt% (4.3 vs. 2.68–3.68) and 10 wt% (8.5 vs. 5.33–5.72) using the same emulsification process, respectively. In the emulsification I series, the SBE dosage correlated posi-

tively with the UVP performance both at the measured SPF and the protection factor of the UVA range (Fig. S20†). With the same SBE dosage, E-II-1% gave a slightly lower protection than E-I-1% (Fig. S20†) which was caused possibly by the thermal instability (temperature of 80 °C) or the pH adjustment in emulsification II. The stilbene glucosides (Fig. 1) and

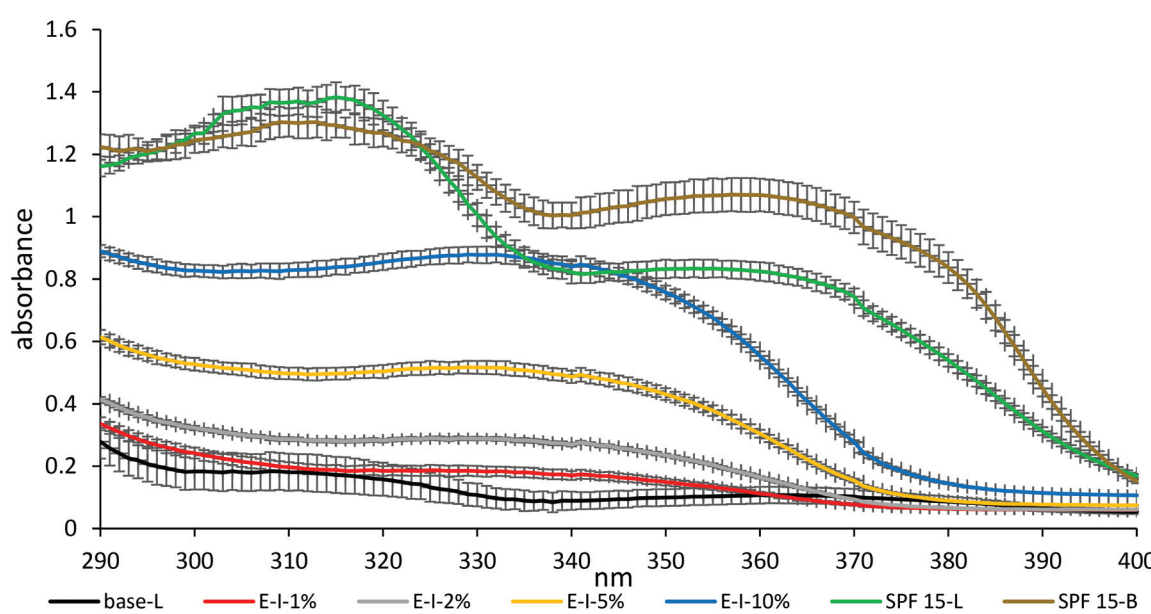


Fig. 7 UVA–UVB (290–400 nm) absorbance of emulsification I (E-I-1%, E-I-2%, E-I-5%, and E-I-10%) in comparison with the commercial creams (base-L; SPF 15-L and SPF 15-B). Their standard deviations are included.



Table 4 The measured SPF/UVA/LOC values before and after solar irradiation

	Solar irradiation	SPF	PF UVA	LOC CW (nm)
Base-L (reference)	Before	1.5	1.3	380
	After	1.4	1.3	381
E-I-1%	Before	1.7	1.4	374
	After	1.3	1.2	380
E-I-2%	Before	2.4	1.6	365
	After	1.6	1.3	371
E-I-5%	Before	4.3	2.1	360
	After	2.2	1.6	365
E-I-10%	Before	8.5	3.0	359
	After	3.7	2.2	364
E-II-1%	Before	1.6	1.4	378
	After	1.5	1.3	380
E-II-2%	Before	1.9	1.5	371
	After	1.5	1.3	376
SPF 15-L (positive control)	Before	16.6	5.7	375
	After	14.9	5.3	375
SPF 15-B (positive control)	Before	16.7	9.7	378
	After	14.4	8.0	378
SPF 30-L (positive control)	Before	36.0	24.5	380
	After	35.8	25.5	380

UVA corresponds to the protection factor of the UVA range. CW is the wavelength below which 90% of the absorbance curve resides. All calculation is based on the average of four independent measurements.

condensed tannins that might be present in SBE are weakly acidic and their ionization changes their light absorption spectra. Interestingly, the visual appearance of E-II-1% was close to that of E-I-10% (Fig. S21†). *trans*-Resveratrol has been reported to be stable for several months when protected from light and kept at neutral pH.⁵⁶ Therefore, a pH adjustment of

the creams may play a role in preserving the stilbene glucosides; however this is out of scope of this present study.

The solar irradiation using a sun simulator allows the determination of the photostability of the tested samples. In the emulsification I series, the SBE dosage correlated negatively with the UVP performance both at the measured SPF and the protection factor of the UVA range. To be specific, the measured SPF increased progressively from 24 to 56% at the dosages of 1–10%, respectively. The low photostability of the stilbene glucosides could be explained by the fact that *trans*-stilbene glucosides may convert into their *cis*-isomers under light and further into phenanthrene under UV irradiation. The major drawbacks of liberating the full biological effects of stilbene glucosides apparently lie in these molecules' poor stability and low solubility. Their use as sunscreen UV-filters is therefore limited to a certain pH and solvent. Besides, the conventional chemical conjugation strategies (e.g. esterification, alkylation, and acylation)^{57,58} could alter the molecule's characters; the enzymatic functionalization like glycosylation⁵⁹ and lipase-catalysed enzymatic acylation⁶⁰ are other alternative biocompatible strategies for solubility and stability enhancement. The suggested reactions shown in Fig. 8 are not listed as part of the 'restricted reaction' to manufacture the naturally derived cosmetic ingredients according to ISO 16128-1.⁶¹ Notably, the solubility of the resveratrol 3,5- β -D-diglucoside improved with 1700-fold more water solubility than the unglucosylated molecule without losing its antioxidant activity.²⁸ Such protection strategies are thought to enhance the stability and hydrophobicity of these compounds at neutral pH and their original colour could be preserved. Thus, (bio)chemical functionalization needs to be systematically carried out to improve the overall stability of stilbene.

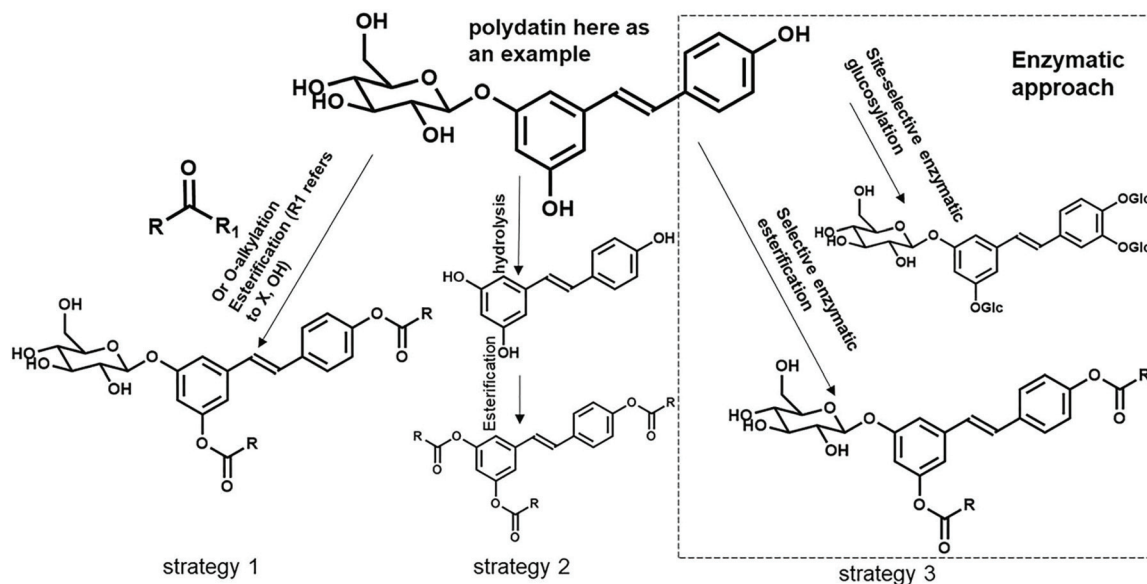


Fig. 8 Possible controlled functionalization of the stilbene glucosides (or their aglycon forms) from spruce bark (polydatin is used as an example). Enzymatic approach is highlighted with a dashed line.



Conclusions

Today, the conventional synthetic UV filters are posing a global public health concern for the environment and humans. They can transmit and have an impact on the survival rate and reproduction of aquatic organisms *via* humans' sunscreen products. Thus, we need to develop alternative safer sunscreens, *e.g.*, new types of naturally derived UV absorbers. A short ultrasound-assisted treatment of spruce inner bark with 60 v% ethanol at 45 °C provided an extract (SBE) that was rich in stilbene glucosides. One- and two-dimensional NMR and LC-MS techniques verified the structure of the main stilbene glucosides, astringin, isorhapontin and polydatin, which together formed one third of the extract and *ca.* 9.0% of the original bark. The extract was brownish in colour which possibly originated from coextracted condensed tannins. A 10% emulsion of SBE (containing 35% stilbene glucosides) provided UV protection equal to half the efficiency of commercial SPF 15 sun lotions. The UV protection performance of spruce bark extracts outperformed that of lignin¹¹ at the same dosages of 5 or 10 wt%.

The spruce bark stilbenes have shown their significant UV-absorbing capacity, but there have not been enough scientific data to enhance their photostability and solubility. A systematic study (Fig. 8) will be conducted to introduce substituted ester functionalities through chemo-enzymatic strategies. The solubility and stability of these functionalized stilbenes may improve 1000-fold with more water solubility without losing their UV-absorbing activity. Currently, spruce bark is entirely for energy use at pulp mills, while this resource-wise use of spruce bark for stilbene in sunscreens will allow more income potential for forest owners. This is the first scientific demonstration of the use of a stilbene-rich spruce bark extract as a UV blocker in sunscreens and it may potentially lead to the commercial utilization of spruce bark in the cosmetic industry. However, it is still quite far from the current preliminary research to a fully medically certified marketable product in the context of 'spruce bark biorefinery'. Further work will also be needed to demonstrate the long-term performance of SBE in the products.

Conflicts of interest

There are no conflicts to declare.

Acknowledgements

Aalto University CHEMARTS is acknowledged as the initiator of the original concept of applying spruce bark extracts as UV protection additives. The authors would like to thank Petri Widsten (VTT), Owain Dawson and Maria Rodriguez (Aalto University), and Jean-Claude HUBAUD (Helioscience) for their skilful assistance in the UV absorbance measurements. Special thanks go to Heidi Henrickson from Aalto University for the

language check. This work is part of the Academy of Finland's Flagship Programme under Project No. 318890 and No. 318891 (Competence Center for Materials Bioeconomy, FinnCERES).

References

- 1 M. F. Bennett, M. K. Robinson, E. D. Baron and K. D. Cooper, *J. Invest. Dermatol. Symp. Proc.*, 2008, **13**, 15–19, DOI: 10.1038/jidsymp.2008.3.
- 2 S. T. Butt and T. Christensen, *Radiat. Prot. Dosim.*, 2000, **91**, 283–286, DOI: 10.1093/oxfordjournals.rpd.a033219.
- 3 E. Gilbert, F. Pirot, V. Bertholle, L. Roussel, F. Falson and K. Padois, *Int. J. Cosmet. Sci.*, 2013, **35**, 208–219, DOI: 10.1111/ics.12030.
- 4 K. Matsumoto, Y. Akao, E. Kobayashi, T. Ito, K. Ohguchi, T. Tanaka, M. Iinuma and Y. Nozawa, *Biol. Pharm. Bull.*, 2003, **26**, 569–571, DOI: 10.1248/bpb.26.569.
- 5 J. A. Ruszkiewicz, A. Pinkas, B. Ferrer, T. V. Peres, A. Tsatsakis and M. Aschner, *Toxicol. Rep.*, 2017, **4**, 245–259, DOI: 10.1016/j.toxrep.2017.05.006.
- 6 Ź. Broniowska, B. Pomierny, I. Smaga, M. Filip and B. Budziszewska, *Neurotoxicology*, 2016, **54**, 44–52, DOI: 10.1016/j.neuro.2016.03.003.
- 7 A. J. Waters, D. R. Sandhu, G. Lowe and J. Ferguson, *Contact Dermatitis*, 2009, **60**, 172–173, DOI: 10.1111/j.1600-0536.2008.01448.x.
- 8 C. A. Downs, E. Kramarsky-Winter, R. Segal, J. Fauth, S. Knutson, O. Bronstein, F. R. Ciner, R. Jeger, Y. Lichtenfeld, C. M. Woodley, P. Pennington, K. Cadenas, A. Kushmaro and Y. Loya, *Arch. Environ. Contam. Toxicol.*, 2016, **70**, 265–288, DOI: 10.1007/s00244-015-0227-7.
- 9 P. K. Goswami, M. Samant and R. Srivastava, *Scholars Acad. J. Pharm.*, 2013, **2**, 458–463.
- 10 E. Hoque and G. Remus, *Photochem. Photobiol.*, 1999, **69**, 177–192, DOI: 10.1111/j.1751-1097.1999.tb03272.x.
- 11 Y. Qian, X. Qiu and S. Zhu, *Green Chem.*, 2015, **17**, 320–324, DOI: 10.1039/C4GC01333F.
- 12 Y. Qian, X. Qiu and S. Zhu, *ACS Sustainable Chem. Eng.*, 2016, **4**, 4029–4035, DOI: 10.1021/acssuschemeng.6b00934.
- 13 D. Blondeau, A. St-Pierre, N. Bourdeau, J. Bley, A. Lajeunesse and I. Desgagné-Penix, *MicrobiologyOpen*, 2020, **9**, e944, DOI: 10.1002/mbo3.944.
- 14 Azelaic Acid at innomost, <https://www.innomost.com/products/azelaic-acid/>, (accessed January 2022).
- 15 H. Gollnick and A. Layton, *Expert Opin. Pharmacother.*, 2008, **9**, 2699–2706, DOI: 10.1517/14656566.9.15.2699.
- 16 K. Kemppainen, M. Siika-aho, S. Pattathil, S. Giovando and K. Kruus, *Ind. Crops Prod.*, 2014, **52**, 158–168, DOI: 10.1016/j.indcrop.2013.10.009.
- 17 T. Jyske, T. Laakso, H. Latva-Mäenpää, T. Tapanila and P. Saranpää, *Biomass Bioenergy*, 2014, **71**, 216–227, DOI: 10.1016/j.biombioe.2014.10.005.
- 18 H. Latva-Mäenpää, T. Laakso, T. Sarjala, K. Wähälä and P. Saranpää, *Trees*, 2013, **27**, 131–139, DOI: 10.1007/s00468-012-0780-x.



19 G. Singh and J. Kumar, artificial and natural photoprotective compounds, in *Sunscreens*, ed. R. P. Rastogi, Nova Science Publisher, New York, 2018, vol. 7, pp. 153–199.

20 J. Gabaston, T. Richard, B. Biais, P. Waffo-Teguo, E. Pedrot, M. Jourdes, M. F. Corio-Costet and J. M. Mérillon, *Ind. Crops Prod.*, 2017, **103**, 267–273, DOI: 10.1016/j.indcrop.2017.04.009.

21 V. R. Franceschi, P. Krokene, E. Christiansen and T. Krekling, *New Phytol.*, 2005, **167**, 353–376, DOI: 10.1111/j.1469-8137.2005.01436.x.

22 M. Reinisalo, A. Kårlund, A. Koskela, K. Kaarniranta and R. O. Karjalainen, *Oxid. Med. Cell. Longevity*, 2015, **2015**, 340520, DOI: 10.1155/2015/340520.

23 A. Freyssin, G. Page, B. Fauconneau and A. R. Bilan, *Neural Regener. Res.*, 2020, **15**, 843–849, DOI: 10.4103/1673-5374.268970.

24 J. Rencoret, D. Neiva, G. Marques, A. Gutiérrez, H. Kim, J. Gominho, H. Pereira, J. Ralph and J. C. del Río, *Plant Physiol.*, 2019, **180**, 1310–1321, DOI: 10.1104/pp.19.00344.

25 B. Fauconneau, P. Waffo-Teguo, F. Huguet, L. Barrier, A. Decendit and J. M. Merillon, *Life Sci.*, 1997, **61**, 2103–2110, DOI: 10.1016/S0024-3205(97)00883-7.

26 S. D. Maria, I. Scognamiglio, A. Lombardi, N. Amodio, M. Caraglia, M. Cartenì, G. Ravagnan and P. Stiuso, *J. Transl. Med.*, 2013, **11**, 264, DOI: 10.1186/1479-5876-11-264.

27 R. Pangeni, J. K. Sahni, J. Ali, S. Sharma and S. Baboota, *Expert Opin. Drug Delivery*, 2014, **11**, 1285–1298, DOI: 10.1517/17425247.2014.919253.

28 A. Lepak, A. Gutmann, S. T. Kulmer and B. Nidetzky, *ChemBioChem*, 2015, **16**, 1870–1874, DOI: 10.1002/cbic.201500284.

29 M. H. Abraham, C. E. Green, W. E. Acree Jr., C. E. Hernandez and L. E. Roy, *J. Chem. Soc., Perkin Trans. 2*, 1998, 2677–2681, DOI: 10.1039/A805769I.

30 F. Silva, A. Figueiras, E. Gallardo, C. Nerín and F. C. Domingues, *Food Chem.*, 2014, **145**, 115–125, DOI: 10.1016/j.foodchem.2013.08.034.

31 J. Qian, M. Hou, X. Wu, C. Dai, J. Sun and L. Dong, *Biomed. Pharmacother.*, 2020, **124**, 109923, DOI: 10.1016/j.biopharm.2020.109923.

32 I. Soural, N. Vrchotová, J. Tříška, J. Balík, Š. Horník, P. Cuřinová and J. Sýkora, *Molecules*, 2015, **20**, 6093–6112, DOI: 10.3390/molecules20046093.

33 H. Latva-Mäenpää, R. Wufu, D. Mulat, T. Sarjala, P. Saranpää and K. Wähälä, *Molecules*, 2021, **26**, 1036, DOI: 10.3390/molecules26041036.

34 Y. J. Cho, J. Y. Hong, H. S. Chun, S. K. Lee and H. Y. Min, *J. Food Eng.*, 2006, **77**, 725–730, DOI: 10.1016/j.jfoodeng.2005.06.076.

35 Z. Piñeiro, A. Marrufo-Curtido, M. J. Serrano and M. Palma, *Molecules*, 2016, **21**, 784, DOI: 10.3390/molecules21060784.

36 J. Krogell, B. Holmbom, A. Pranovich, J. Hemming and S. Willföör, *Nord. Pulp Pap. Res. J.*, 2012, **27**, 6–17, DOI: 10.3183/npprj-2012-27-01-p006-017.

37 IFF Lucas Meyer Sustainably Sources from the Forest, <https://www.cosmeticsandtoiletries.com/cosmetic-ingredi-ents/actives/news/21841054/lucas-meyer-cosmetics-iff-lucas-meyer-sustainably-sources-from-the-forest>, (accessed January 2022).

38 Black Spruce Bark Extract, Vitamin B5 & E Hair Mask for Colored & Treated Hair, <https://www.buywow.in/products/wow-skin-science-hair-mask-for-colored-treated-hair-200ml>, (accessed January 2022).

39 M. Sui, Master thesis, *Spruce bark extract as a sun protection agent in sunscreens*, Aalto University, 2018.

40 A. Semenzato, A. Costantini, M. Meloni, G. Maramaldi, M. Meneghin and G. Baratto, *Cosmetics*, 2018, **5**, 59, DOI: 10.3390/cosmetics5040059.

41 J. Hubaud, D. Guerin, M. D. Salvo, J. E. Branka, K. Mekideche and P. Piccerelle Pr, *J. Cosmet., Dermatol. Sci. Appl.*, 2021, **11**, 253–262, DOI: 10.4236/jcdsa.2021.113021.

42 A. F. McKinley and B. L. Diffey, *CIE J.*, 1987, **6**, 17–22.

43 J. Dou, H. Kim, Y. Li, D. Padmakshan, F. Yue, J. Ralph and T. Vuorinen, *J. Agric. Food Chem.*, 2018, **66**, 7294–7300, DOI: 10.1021/acs.jafc.8b02014.

44 D. G. Mulat, H. Latva-Mäenpää, H. Koskela, P. Saranpää and K. Wähälä, *Phytochem. Anal.*, 2014, **25**, 529–536, DOI: 10.1002/pca.2523.

45 J. B. Sluiter, R. O. Ruiz, C. J. Scarlata, A. D. Sluiter and D. W. Templeton, *J. Agric. Food Chem.*, 2010, **58**, 9043–9053, DOI: 10.1021/jf1008023.

46 J. Dou, W. Xu, J. J. Koivisto, J. K. Mobley, D. Padmakshan, M. Kögler, C. Xu, S. Willföör, J. Ralph and T. Vuorinen, *ACS Sustainable Chem. Eng.*, 2018, **6**, 5566–5573, DOI: 10.1021/acsuschemeng.8b00498.

47 A. Belay, K. Ture, M. Redi and A. Asfaw, *Food Chem.*, 2008, **108**, 310–315, DOI: 10.1016/j.foodchem.2007.10.024.

48 S. Barbini, D. Sriranganadane, S. E. Orozco, A. Kabrelian, K. Karlström, T. Rosenau and A. Potthast, *ACS Sustainable Chem. Eng.*, 2021, **9**, 1323–1332, DOI: 10.1021/acsuschemeng.0c07914.

49 S. Barbini, J. Jaxel, K. Karlström, T. Rosenau and A. Potthast, *Bioresour. Technol.*, 2021, **341**, 125862, DOI: 10.1016/j.biortech.2021.125862.

50 J. Dou, J. Heinonen, T. Vuorinen, C. Xu and T. Sainio, *Sep. Purif. Technol.*, 2021, **261**, 118247, DOI: 10.1016/j.seppur.2020.118247.

51 B. Fan, W. Dong, T. Chen, J. Chu and B. He, *Org. Biomol. Chem.*, 2018, **16**, 2464–2469, DOI: 10.1039/C8OB00376A.

52 G. F. Pauli, T. Gödecke, B. U. Jaki and D. C. Lankin, *J. Nat. Prod.*, 2012, **75**, 834–851, DOI: 10.1021/np200993k.

53 M. A. Zarin, H. Y. Wan, A. Isha and N. Armania, *Food Sci. Hum. Wellness*, 2016, **5**, 65–75, DOI: 10.1016/j.fshw.2016.02.001.

54 A. Hammerbacher, D. Kandasamy, C. Ullah, A. Schmidt, L. P. Wright and J. Gershenzon, *Front. Plant Sci.*, 2019, **10**, 208, DOI: 10.3389/fpls.2019.00208.

55 S. P. Pietarinen, S. M. Willföör, M. O. Ahotupa, J. E. Hemming and B. R. Holmbom, *J. Wood Sci.*, 2006, **52**, 436–444, DOI: 10.1007/s10086-005-0780-1.



56 B. C. Trela and A. L. Waterhouse, *J. Agric. Food Chem.*, 1996, **44**, 1253–1257, DOI: 10.1021/jf9504576.

57 A. Mattarei, M. Azzolini, M. Carraro, N. Sassi, M. Zoratti, C. Paradisi and L. Biasutto, *Mol. Pharmaceutics*, 2013, **10**, 2781–2792, DOI: 10.1021/mp400226p.

58 M. Larrosa, J. Tomé-Carneiro, M. J. Yáñez-Gascón, D. Alcántara, M. V. Selma, D. Beltrán, M. T. García-Conesa, C. Urbán, R. Lucas, F. Tomás-Barberán, J. C. Morales and J. C. Espín, *J. Med. Chem.*, 2010, **53**, 7365–7376, DOI: 10.1021/jm1007006.

59 G. Regev-shoshani, O. Shoseyov, I. Bilkis and Z. Kerem, *Biochem. J.*, 2003, **374**, 157–163, DOI: 10.1042/BJ20030141.

60 P. Torres, A. Poveda, J. Jimenez-Barbero, A. Ballesteros and F. J. Plou, *J. Agric. Food Chem.*, 2010, **58**, 807–813, DOI: 10.1021/jf903210q.

61 ISO 16128-1:2016. Guidelines on technical definitions and criteria for natural and organic cosmetic ingredients and products, <https://www.iso.org/standard/62503.html>, (accessed January 2022).

